Ab initio Determination of the Phase Diagram of CO_2 at High Pressures and Temperatures

Beatriz H. Cogollo-Olivo,[1,*] Sananda Biswas,[2] Sandro Scandolo,[3] and Javier A. Montoya[4]
[1]*Universidad de Cartagena, Doctorado en Ciencias Físicas, 130001 Cartagena de Indias, Colombia*
[2]*Institut für Theoretische Physik, Goethe-Universität Frankfurt, 60438 Frankfurt am Main, Germany*
[3]*The Abdus Salam International Centre for Theoretical Physics (ICTP), Strada Costiera 11, 34151 Trieste, Italy*
[4]*Universidad de Cartagena, Instituto de Matemáticas Aplicadas, 130001 Cartagena de Indias, Colombia*

(Received 25 October 2019; accepted 10 February 2020; published 2 March 2020)

The experimental study of the CO_2 phase diagram is hampered by strong kinetic effects leading to wide regions of metastability and to large uncertainties in the location of some phase boundaries. Here, we determine CO_2's thermodynamic phase boundaries by means of *ab initio* calculations of the Gibbs free energy of several solid phases of CO_2 up to 50 Gigapascals. Temperature effects are included in the quasiharmonic approximation. Contrary to previous suggestions, we find that the boundary between molecular forms and the nonmolecular phase V has, indeed, a positive slope and starts at 21.5 GPa at $T = 0$ K. A triple point between phase IV, V, and the liquid phase is found at 35 GPa and 1600 K, indicating a broader region of stability for the nonmolecular form than previously thought. The experimentally determined boundary line between CO_2-II and CO_2-IV phases is reproduced by our calculations, indicating that kinetic effects do not play a major role in that particular transition. Our results also show that CO_2-III is stabilized at high temperature and its stability region coincides with the *P-T* conditions where phase VII has been reported experimentally; instead, phase II is the most stable molecular phase at low temperatures, extending its region of stability to every *P-T* condition where phase III is reported experimentally.

DOI: 10.1103/PhysRevLett.124.095701

Widely studied during the past years, carbon dioxide (CO_2) is a fascinating system that, despite its simple molecular form at ambient conditions, exhibits a rich polymorphism at high pressures and temperatures, with up to seven crystalline structures reported experimentally so far, in addition to an amorphous form (see Fig. 1). At room temperature the molecular gas transforms into a liquid at 7.5 MPa which then solidifies at 0.5 GPa into CO_2-I, a molecular crystal with space group $Pa\bar{3}$ [1,2]. By further increasing pressure at ambient temperature, CO_2-I transforms to the orthorhombic phase III (*Cmca* space group) above 10 GPa, with a minimal volume change [3]. A recent theoretical study has provided insights into the microscopic mechanism of the $Pa\bar{3}$-to-*Cmca* transition [4]. Heating compressed CO_2-III above ~470 K [5,6] leads to the transformation into phase II. However, this transition is not reversible: CO_2-II can be recovered at ambient temperature while pressurized, suggesting that CO_2-III is a kinetic product of the compression of CO_2-I and not a stable phase [5,7]. With the exception of a recent theoretical study [8], all previous theoretical work confirms that CO_2-II is more stable than CO_2-III at ambient temperature and below. Initially described as a structure with carbon in an unconventional sixfold coordination, phase II was interpreted as an intermediate state between the molecular and the extended solid form of CO_2 [9], however, subsequent studies disproved the existence of such an intermediate bonding state and identified the structure of phase II as composed of undistorted molecules, with space group $P4_2/mnm$ [10]. CO_2-II transforms into CO_2-IV when it is heated in the 500–720 K range, depending on

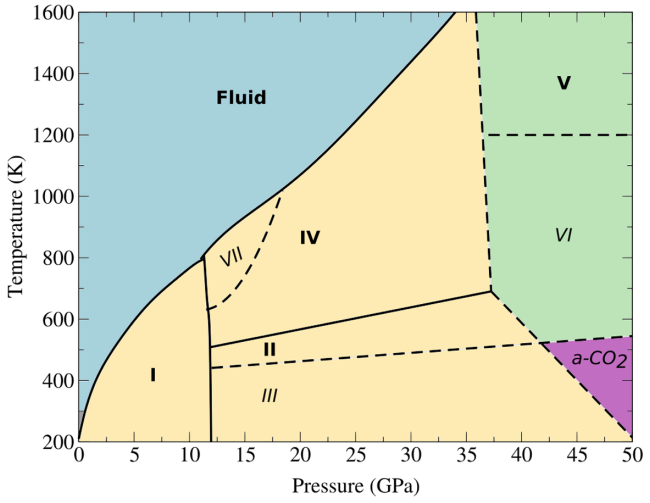

FIG. 1. CO_2 phase diagram adapted from Ref. [15]. Yellow, green, blue, and purple areas correspond to the molecular, nonmolecular, fluid, and amorphous forms of CO_2, respectively. Solid lines correspond to thermodynamic phase boundaries, while dashed lines are kinetic boundaries. Names in bold and italic indicate thermodynamic and metastable phases, respectively.

pressure [5,7]. Phase IV, similar to phase II, was also initially interpreted as an intermediate bonding state [11]; here again, this interpretation was disproved by showing experimentally that CO_2-IV is still composed of well defined linear molecules and that its crystalline structure is rhombohedral with space group $R\bar{3}c$ [12]. At higher temperatures, an intermediate phase between CO_2-I and CO_2-IV was observed by heating CO_2-I to ~950 K and compressing it up to 20 GPa. The crystal structure of this molecular high-temperature stable phase (CO_2-VII) belongs to space group *Cmca*. [13]. Despite the fact that CO_2-VII and CO_2-III have the same space group, some differences in their Raman spectra and in their lattice parameters suggested that their structures might be quantitatively and qualitatively different [13]. However, a recent theoretical study has shown that CO_2-III and CO_2-VII belong to the same configurational energy minimum and that CO_2-III is a low temperature metastable manifestation of CO_2-VII [14].

The nonmolecular CO_2-V phase was first synthesized by laser heating CO_2-III above 40 GPa and 1800 K [16], and its crystalline structure has now been determined as a fully tetrahedral partially collapsed cristobalitelike structure, with space group $I\bar{4}2d$ [17,18]. By compressing CO_2-II to 50 GPa at 530 and 650 K, another nonmolecular form of carbon dioxide (CO_2-VI) was obtained [11]. Its vibrational spectra is consistent with those of metastable layered tetrahedral structures, as shown in [19]. In addition to the molecular and nonmolecular phases, an amorphous form of carbon dioxide (a-CO_2) was observed upon compressing CO_2-III in the pressure range from 40 to 48 GPa at room temperature [7]. The microscopic structure of a-CO_2 has been explained as a frustrated mixture of threefold and fourfold coordinated carbon atoms, in an intermediate metastable form towards fully tetrahedral coordination [20]. Finally, CO_2-V has been reported to dissociate into elemental carbon (diamond) and oxygen ($\epsilon - O_2$) at pressures between 30 and 80 GPa, and temperatures above 1700 K, [21,22]. However, more recent theoretical [23] and experimental [24] works have not observed a transition from the nonmolecular CO_2-V phase into a dissociated state. Moreover, Dziubek *et al.* [24] confirmed that CO_2-V is the only stable phase among all known nonmolecular forms of carbon dioxide, as already proposed by a previous experimental work [25] as well as by theoretical structural searches in the previous decade. The fate of CO_2 at high pressures has important implications for the Earth's global carbon budget [26]. CO_2 degassing in the upper mantle affects melting beneath oceanic ridges [27] and carbonate decomposition [28] may have implications for plume formation in the lower mantle [29]. Therefore, a precise assessment of the transition lines between CO_2 phases, can offer a better understanding of the dynamics of CO_2 within the context of the deep carbon cycle. The goal of defining a complete thermodynamic phase diagram for this basic molecular system has been elusive to experimentalists due to the unique and incredibly strong kinetic limitations and the metastability that are present in CO_2's molecular and extended forms, this, in addition to diverse interpretations of the experimental diffraction data coming from very small samples in diamond anvil cell (DAC) experiments. It is, then, problematic that, after many decades of research, there is no final thermodynamic phase diagram for CO_2 in a range of *P-T* conditions that have been accessible in the lab by diamond anvil cell experiments since the end of the previous century. In this sense, by avoiding uncertainties coming from kinetic limitations and metastability, our Letter presents a well motivated purely *ab initio* density functional theory (DFT)-based determination of the complete phase diagram of CO_2 in an ample pressure and temperature range.

The currently accepted phase diagram including all the mentioned forms of solid CO_2 along with the region where it becomes a fluid is shown in Fig. 1.

In this particular system, strong kinetic effects hinder the experimental determination of the phase boundaries, while the small size of the samples in high-pressure experiments makes structure determinations quite difficult. As a consequence, several questions remain open regarding the nature and location of the phase boundaries and the stability of the phases reported in Fig. 1. In the molecular portion of the phase diagram, open questions include the relative stability of CO_2-II and CO_2-III at low temperature, and the nature of CO_2-VII, in particular its structural relationship with CO_2-III. At higher pressures, one of the fundamental questions is the location of the phase boundary between molecular and nonmolecular phases. Santoro *et al.*, for example, proposed a phase diagram where the boundary between molecular and nonmolecular phases at room temperature is located at 20 GPa, roughly half-way between the lowest pressure of quenching and the pressure of synthesis for this phase [30,31]. Moreover, the kinetic boundary between CO_2-III and the a-CO_2 nonmolecular structure, i.e., the *P-T* region where the transformation occurs upon compression, has a negative slope [32], while basic thermodynamic considerations suggest that the slope of the true phase boundary should be positive [31]. Theoretical determinations of the molecular-nonmolecular boundary at zero temperature, based on *ab initio* electronic structure methods, predict transition pressures in the range between 18 and 21 GPa when going from both CO_2-II and CO_2-III to the nonmolecular forms [28,30,33].

In this Letter, we extend the theoretical determination of the phase diagram of CO_2 to finite temperatures for all stable phases except CO_2-I. Phase boundaries between the molecular phases II, III, and IV, and the nonmolecular phase V are calculated based on an *ab initio* approach; for the determination of free energies, the vibrational contributions are treated in the quasiharmonic approximation (QHA).

Ab initio electronic structure calculations were carried out using DFT and the projector augmented wave method, as implemented in the Quantum ESPRESSO suite [34,35] with a kinetic energy cutoff of 200 Ry for the plane-wave basis set. The generalized gradient approximation was employed for the exchange-correlation energy and implemented using the Perdew-Burke-Ernzerhof functional [36]. Our system is well represented by this approach as shown by previously calculated intramolecular C = O bond lengths of CO_2-II at different levels of theory, which are generally consistent with our values [14,37,38]. The Monkhorst-Pack method [39] was used to generate the k point grids for sampling the Brillouin zone. Variable-cell optimization of all structural parameters was performed for the four phases in the range of pressures between 10 and 70 GPa. Density functional perturbation theory within the linear response scheme [40] was used to calculate phonon frequencies at zero temperature. The zero-point energy and the finite-temperature contributions to the Helmholtz free energy were computed in the QHA [41,42], which is valid where harmonic effects dominate the material's properties. It is commonly accepted as a criterion that increasingly relevant contributions coming from anharmonicities are expected to appear at $T \sim 1.2\Theta_D$ and above [43,44]. Even more, the range of temperatures in which QHA remains valid is significantly expanded under high pressure [43–45]. For this particular study, the calculated Θ_D takes values between 3485 K and 3500 K for the three molecular forms considered at the lowest pressure in our work (10 GPa), which are clearly higher than the highest temperature registered in this study, i.e., 1600 K. Thus, the temperature region under consideration in this work spans approximately from 0.05 to $0.45\Theta_D$, assuring us of the validity of the quasiharmonic approximation below the melting curve of CO_2 for all solid forms. For the construction of the pressure-temperature phase diagram, the Helmholtz free energy at different temperatures was fitted to a third order Birch-Murnaghan equation of state (EOS). Finally, the Gibbs free energy was calculated as

$$G(P,T) = F[V(P,T),T] + PV(P,T), \qquad (1)$$

Room-temperature equations of state obtained with the above approximations are compared with experimental data for phases CO_2-II, CO_2-III, CO_2-IV, and CO_2-V in Fig. 2. The agreement is good and confirms the validity of the approach. Phase boundaries constructed based on the calculated Gibbs free energies are shown in Fig. 3. It is worth mentioning that although most phases in this study are molecular, the van der Waals approximation was not used since, in simulations under very high pressure, the dispersion function becomes constant at distances much shorter than the standard van der Waals radii, resulting in not affecting the valence geometries or energies [46,47].

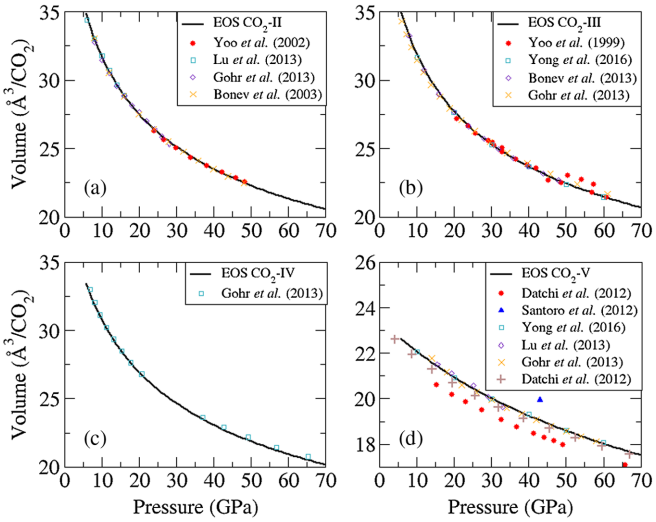

FIG. 2. Pressure-volume relation of phases (a) II, (b) III, (c) IV, and (d) V of CO_2 at room temperature are shown in black solid lines. For each case, reported values from experimental (red circles) and theoretical (blue squares, purple diamonds, and yellow crosses) studies for the different phases are displayed as well.

We begin our discussion with an analysis of the molecular solid region of the phase diagram. This region is indicated in yellow in Fig. 1; it contains the molecular phases I, II, III, and IV, and its upper bound in pressure coincides with the experimentally reported transitions to the nonmolecular phases. Since phase I as well as its boundaries with the other phases are well known and constrained, we focus specifically on phases II, III, and IV, at pressures higher than 12 GPa. According to the enthalpy-pressure relations, with and without the zero-point energy contribution, at $T = 0$ K CO_2-II is the most stable molecular phase in the pressure range considered, until the transition to CO_2-V. This indicates that the orthorhombic *Cmca* structure (phase III) obtained experimentally from the compression of phase I is, indeed, only metastable at low temperatures. Notice that this remains true even after the inclusion of zero-point contributions, in agreement with previous reports [5,48]. At variance with our results as well as with previous theoretical work, a recent theoretical study [8] proposes a transition boundary between phases II and III in which CO_2-III is stable up to ~570 K at 19 GPa. This is at odds with experimental observations where the kinetic transition from CO_2-III to CO_2-II occurs at much lower temperatures [5]. Instead, our calculations show that CO_2-III becomes more stable than CO_2-II at higher temperatures [solid green line with stars in Fig. 3(a)]. The transition temperature between CO_2-III and CO_2-II has a strong pressure dependence and reaches values in excess of 1000 K close to the boundary with the nonmolecular phase V, with respect to its value close to CO_2-I. Comparing the free energies of CO_2-II and CO_2-IV, we find that the boundary between phases II and IV [solid brown line with down triangles in Fig. 3(a)] agrees quite well with

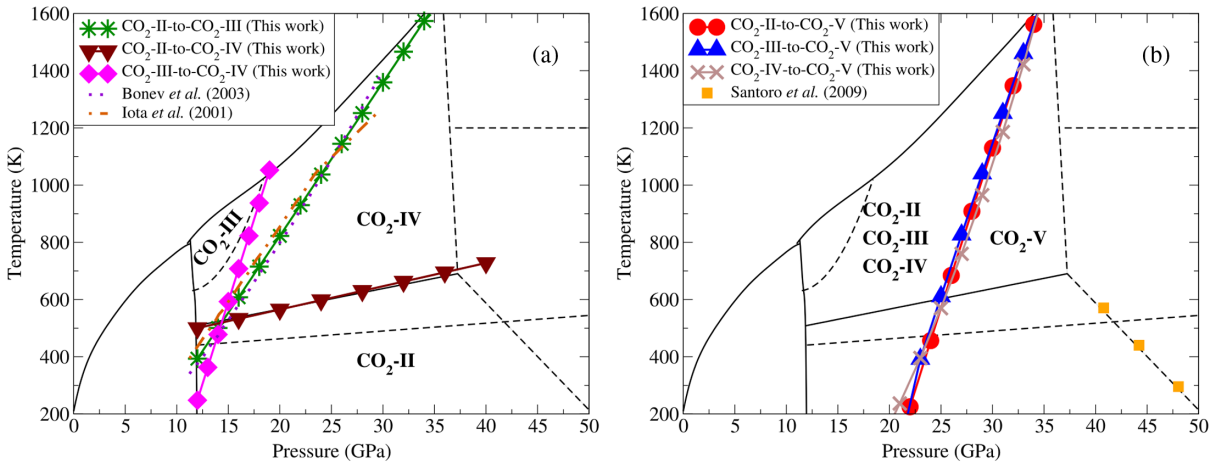

FIG. 3. (a) Phase boundaries between CO_2-II and CO_2-III (green, stars), CO_2-II and CO_2-IV (brown, down triangles), and CO_2-III and CO_2-IV (magenta, diamonds). Suggested boundaries reported by Iota *et al.* [5] (experimental) and Bonev *et al.* [48] (theoretical), are shown in orange dotted-dashed line and violet dotted line, respectively. (b) Phase boundaries between molecular phases CO_2-II (red, circles), CO_2-III (blue, up triangles), and CO_2-IV (gray, crosses), and the nonmolecular phase CO_2-V. Proposed limits of the kinetic region from experimental data from Ref. [32] (orange squares) are also included.

experimental data [12]. The weak pressure dependence of the II-IV boundary reduces the region of stability of phase II with respect to the starred green line in Fig. 3(a), by confining it toward lower temperatures. Finally, we find that the boundary between CO_2-III and CO_2-IV [solid magenta line with diamonds in Fig. 3(a)] is almost vertical, which restricts the domain of stability of phase III to a narrow window of pressure and to temperatures above 400 K. We summarize the results of the free-energy calculations for the three molecular phases II, III, and IV in Fig. 4. Phases I and II emerge as the only stable molecular phases of CO_2 from zero to ambient temperature. Phases III and IV are both stabilized by temperature, and phases II, III, and IV coexist at a triple point located at 15 GPa and 500 K.

Our findings are in agreement with simulations by Bonev *et al.* [48] which suggested that the *Cmca* phase is a temperature stabilized form [48]. Because the structure of phase IV was not known at the time, Bonev *et al.* proposed a wider region of stability for CO_2-III. Interestingly, as can be seen in Fig. 3(a), the *P-T* region of stability of CO_2-III obtained from our calculations has a large overlap with the region of stability reported for the so-called phase VII of CO_2 [13]. A recent theoretical work has shown that phases III and VII have, in fact, the same crystal structure (space group *Cmca*)[14]. Therefore, we confirm that phase III is thermodynamically stable in the *P-T* region where phase VII has been reported. Thus, the observation of phase III outside this region (e.g., at ambient conditions, as a result of the compression of phase I) must be attributed to kinetic effects.

Now, we turn to the boundary between the molecular phases and nonmolecular phase V [Fig. 3(b)]. We find that, at zero temperature, the phase boundary between CO_2-II and CO_2-V is located at 21.5 GPa. The transition between (metastable) CO_2-III and CO_2-V would, instead, take place at 20.8 GPa in the absence of kinetic effects. This is in good agreement with previous theoretical works [28,30,33]. Phase boundaries between molecular phases and CO_2-V are rather insensitive to the choice of the molecular structure and they all have a positive slope, as already suggested [31]. Considering that nonmolecular phases are denser than molecular ones, a positive slope implies a decrease of entropy in going from molecular to nonmolecular. This is not unexpected, given the stiffness of

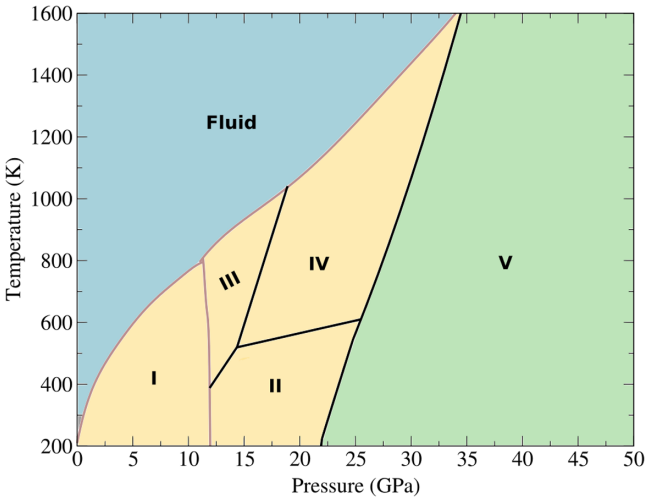

FIG. 4. Theoretical phase diagram for carbon dioxide at high pressure and temperature. Our calculated phase boundaries are shown with solid black lines, while previously reported thermodynamic boundaries are shown in gray. Yellow, green, and blue regions correspond to molecular, nonmolecular, and fluid forms of CO_2.

the nonmolecular structure when compared with the molecular ones. Using the experimentally determined melting line, our calculations show a triple point between phases IV and V, and the liquid phase at 35 GPa and 1600 K. Therefore, the calculations suggest that molecular CO_2 could be stable up to pressures as high as 35 GPa, at high temperature.

In summary, we have presented finite-temperature theoretical calculations in the quasiharmonic approximation for various molecular and nonmolecular solid forms of CO_2. The calculations aimed at resolving experimental uncertainties and inconsistencies due to kinetic effects and metastability. We find that the boundary between the molecular phases and phase V has a positive slope, and starts at 21.5 GPa at $T = 0$ K. We also find that the phase diagram shows a triple point between phases IV, V, and the liquid phase at 35 GPa and 1600 K. This indicates that the nonmolecular phase V has a broader region of stability than previously reported. We were able to reproduce the known thermodynamic boundary line between CO_2-II and CO_2-IV, confirming that kinetic effects are not relevant in that transition. Finally, it was shown that phase II is the most stable molecular phase at low temperatures, extending its region of stability to every P-T condition where phase III has been reported experimentally. However, our results also show that CO_2-III is, instead, stabilized at high temperature and its stability region coincides with the P-T conditions where phase VII has been reported experimentally, implying that phase III and phase VII are, indeed, the same.

We acknowledge the ISCRA Program of CINECA for provision of computational time under Grant No. HP10CVCDOB. B. H. C.-O. thanks Becas Doctorales COLCIENCIAS for support (Grants No. 647-2016 and No. FP44842-299-2016); also, support from the ICTP STEP Programme is gratefully acknowledged. J. A. M. thanks the Vicerrectoría de Investigaciones of the Universidad de Cartagena, for the support of the Grupo de Modelado Computacional through internal grants.

*bcogolloo@unicartagena.edu.co

[1] A. Simon and K. Peters, Acta Crystallogr. Sect. B **36**, 2750 (1980).
[2] R. T. Downs and M. S. Somayazulu, Acta Crystallogr. Sect. C **54**, 897 (1998).
[3] K. Aoki, H. Yamawaki, M. Sakashita, Y. Gotoh, and K. Takemura, Science **263**, 356 (1994).
[4] I. Gimondi and M. Salvalaglio, J. Chem. Phys. **147**, 114502 (2017).
[5] V. Iota and C. S. Yoo, Phys. Rev. Lett. **86**, 5922 (2001).
[6] F. A. Gorelli, V. M. Giordano, P. R. Salvi, and R. Bini, Phys. Rev. Lett. **93**, 205503 (2004).
[7] M. Santoro, F. A. Gorelli, R. Bini, G. Ruocco, S. Scandolo, and W. A. Crichton, Nature (London) **441**, 857 (2006).
[8] Y. Han, J. Liu, L. Huang, X. He, and J. Li, npj Quantum Mater. **4**, 10 (2019).
[9] C. S. Yoo, H. Kohlmann, H. Cynn, M. F. Nicol, V. Iota, and T. LeBihan, Phys. Rev. B **65**, 104103 (2002).
[10] F. Datchi, B. Mallick, A. Salamat, G. Rousse, S. Ninet, G. Garbarino, P. Bouvier, and M. Mezouar, Phys. Rev. B **89**, 144101 (2014).
[11] V. Iota, C. S. Yoo, J. H. Klepeis, Z. Jenei, W. Evans, and H. Cynn, Nat. Mater. **6**, 34 (2007).
[12] F. Datchi, V. M. Giordano, P. Munsch, and A. M. Saitta, Phys. Rev. Lett. **103**, 185701 (2009).
[13] V. M. Giordano and F. Datchi, Europhys. Lett. **77**, 46002 (2007).
[14] W. Sontising, Y. N. Heit, J. L. McKinley, and G. J. O. Beran, Chem. Sci. **8**, 7374 (2017).
[15] F. Datchi, G. Weck, A. M. Saitta, Z. Raza, G. Garbarino, S. Ninet, D. K. Spaulding, J. A. Queyroux, and M. Mezouar, Phys. Rev. B **94**, 014201 (2016).
[16] V. Iota, C. S. Yoo, and H. Cynn, Science **283**, 1510 (1999).
[17] M. Santoro, F. A. Gorelli, R. Bini, J. Haines, O. Cambon, C. Levelut, J. A. Montoya, and S. Scandolo, Proc. Natl. Acad. Sci. U.S.A. **109**, 5176 (2012).
[18] F. Datchi, B. Mallick, A. Salamat, and S. Ninet, Phys. Rev. Lett. **108**, 125701 (2012).
[19] M. S. Lee, J. A. Montoya, and S. Scandolo, Phys. Rev. B **79**, 144102 (2009).
[20] J. A. Montoya, R. Rousseau, M. Santoro, F. Gorelli, and S. Scandolo, Phys. Rev. Lett. **100**, 163002 (2008).
[21] O. Tschauner, H. K. Mao, and R. J. Hemley, Phys. Rev. Lett. **87**, 075701 (2001).
[22] K. D. Litasov, A. F. Goncharov, and R. J. Hemley, Earth Planet. Sci. Lett. **309**, 318 (2011).
[23] A. Teweldeberhan, B. Boates, and S. Bonev, Earth Planet. Sci. Lett. **373**, 228 (2013).
[24] M. Dziubek, Kamil F. Ende, D. Scelta, R. Bini, M. Mezouar, G. Garbarino, and R. Miletich, Nat. Commun. **9**, 3148 (2018).
[25] Y. Seto, D. Nishio-Hamane, T. Nagai, N. Sata, and K. Fujino, J. Phys. Conf. Ser. **215**, 012015 (2010).
[26] R. M. Hazen, A. P. Jones, and J. A. Baross, Rev. Mineral. Geochem. **75** (2013), http://www.minsocam.org/msa/rim/rim75.html.
[27] R. Dasgupta, A. Mallik, K. Tsuno, A. C. Withers, G. Hirth, and M. M. Hirschmann, Nature (London) **493**, 211 (2013).
[28] A. R. Oganov, S. Ono, Y. Ma, C. W. Glass, and A. Garcia, Earth Planet. Sci. Lett. **273**, 38 (2008).
[29] N. Takafuji, K. Fujino, T. Nagai, Y. Seto, and D. Hamane, Phys. Chem. Miner. **33**, 651 (2006).
[30] X. Yong, H. Liu, M. Wu, Y. Yao, J. S. Tse, R. Dias, and C. S. Yoo, Proc. Natl. Acad. Sci. U.S.A. **113**, 11110 (2016).
[31] M. Santoro, J. F. Lin, H. K. Mao, and R. J. Hemley, J. Chem. Phys. **121**, 2780 (2004).
[32] M. Santoro and F. A. Gorelli, Phys. Rev. B **80**, 184109 (2009).
[33] S. Gohr, S. Grimme, T. Shnel, B. Paulus, and P. Schwerdtfeger, J. Chem. Phys. **139**, 174501 (2013).
[34] P. Giannozzi *et al.*, J. Phys. Condens. Matter **21**, 395502 (2009).

[35] P. Giannozzi *et al.*, J. Phys. Condens. Matter **29**, 465901 (2017).
[36] J. P. Perdew, K. Burke, and M. Ernzerhof, Phys. Rev. Lett. **77**, 3865 (1996).
[37] J.-H. Parq, S. K. Lee, S.-M. Lee, and J. Yu, J. Phys. Chem. C **120**, 23152 (2016).
[38] H. S. Yu, X. He, and D. G. Truhlar, J. Chem. Theory Comput. **12**, 1280 (2016).
[39] J. D. Pack and H. J. Monkhorst, Phys. Rev. B **16**, 1748 (1977).
[40] S. Baroni, S. de Gironcoli, A. Dal Corso, and P. Giannozzi, Rev. Mod. Phys. **73**, 515 (2001).
[41] G. Leibfried and W. Ludwig, Solid State Phys. **12**, 275 (1961).
[42] S. Baroni, P. Giannozzi, and E. Isaev, Rev. Mineral. Geochem. **71**, 39 (2010).
[43] R. J. Angel, F. Miozzi, and M. Alvaro, Minerals **9**, 562 (2019).
[44] O. Anderson, *Equations of State of Solids for Geophysics and Ceramic Science* (Oxford University Press, New York, 1995).
[45] R. J. Hardy, J. Geophys. Res. **85**, 7011 (1980).
[46] A. Hu, N. Chan, S. Wang, and F. Zhang, Phys. Lett. A **383**, 666 (2019).
[47] Y. Liu and W. A. Goddard, J. Phys. Chem. Lett. **1**, 2550 (2010).
[48] S. A. Bonev, F. Gygi, T. Ogitsu, and G. Galli, Phys. Rev. Lett. **91**, 065501 (2003).